Egyptian Journal of Chemistry

http://ejchem.journals.ekb.eg/

Zeolitic Polyacrylamide Hydrogel for Methylene Blue Removal

Basant A. Elsebai [a], Ahmed F. Ghanem [b,*], Shimaa M. Abdel Moniem [a], Abdelrahman A. Badawy [c], Hanan S. Ibrahim [a], Mostafa M. H. Khalil[d]

[a] *Water Pollution Research Department, Environmental and Climate Changes Institute, National Research Centre, 33 El Bohouth St. (former El Tahrir St.), P.O. 12622, Dokki, Giza, Egypt*

[b] *Packaging Materials Department, Chemical Industries Research Institute, National Research Centre, 33 El Bohouth St. (former El Tahrir St.), P.O. 12622, Dokki, Giza, Egypt*

[c] *Physical Chemistry Department, Advanced Materials Technology and Mineral Resources Research Institute, 33 El Bohouth St. (former El Tahrir St.), P.O. 12622, Dokki, Giza, Egypt*

[d] *Chemistry Department, Faculty of Science, Ain Shams University, 11566. Abbassia, Cairo, Egypt.*

Abstract

In this work, a composite hydrogel based on polyacrylamide and sodium zeolite particles was prepared. Particularly, Na-A zeolite particles were obtained in the alkaline medium via the crystallization of Egyptian kaolin under hydrothermal conditions. Meanwhile, the composite polyacrylamide hydrogel was prepared via an in-situ polymerization approach with different zeolite ratios using acrylamide as a commercial monomer in the presence of an initiator and a crosslinker. The formed modified hydrogel was investigated and compared with the pristine one by several characterization techniques such as Fourier transform infrared (FTIR), X-ray diffraction (XRD), scanning electron microscope (SEM), and gas sorption. The results emphasized the successful preparation and the incorporation of zeolite particles in the hydrogel matrix supporting a strong interaction as well. Application of the prepared composite hydrogel on the removal of methylene blue displayed a superior performance over the pure matrix as the removal percentage reached ~ 96 % after 2 minutes of treatment thanks to improved properties in the presence of zeolite crystals. Adsorption isotherm and kinetic models emphasized that the adsorption reaction is pseudo-second-order and obeys Langmuir. Moreover, thermodynamic studies proved the exothermic reaction as well as the strong interaction between the dye molecules and the gel's surface could be established. Also, the reaction conditions were optimized. The study showed that the superlative parameters in terms of the contact time, the hydrogel weight, pH, temperature, the initial dye concentrations, and even the filler ratios were 30 min., 0.4 g (dried gel), normal, room atmosphere, 50 ppm, and 10 *wt.* %, respectively. Finally, the obtained composite matrix could be reused up to five cycles. It could be claimed that the developed zeolitic hydrogel can pave the way towards a new generation of adsorbents as it is considered a promising candidate in wastewater treatment applications.

Keywords: Hydrogels; Zeolites; Polymer composites; Water treatment.

1. Introduction

Hydrogels (HGs) are considered one of the most efficient adsorbents in water treatment applications [1]. Structurally, the hydrogel is a three-dimensional reticulated network of a hydrophilic polymer in which its chains are cross-linked in the aqueous solution [2]. This leads to holding a high amount of water after formation, greater than 1000 times the polymer mass, which emphasizes the high swelling capacity of these materials [3]. Particularly, hydrogels exhibited high performance in the removal of a broad class of water pollutants including dyes, heavy metals, and organic toxins thanks to their intriguing physicochemical properties [1]. Usually, water-holding gel materials are characterized by unique surface chemistry as versatile functional groups, like -OH, -COOH, - NH_2, and epoxy, are propagated densely on the polymer backbone in the bulk and on the matrix's surface [4]. Moreover, HGs enjoy specific surface textures in terms of high surface area, high porosity, and high total pore volume [5, 6]. These remarkable features promote hydrogels as the best choice for the removal of contaminants from wastewater.

Among the common synthetic hydrogels, polyacrylamide (PCM) is a high molecular weight polymer that can be formulated as a soft gel easily via polymerization of acrylamide, a commercial monomer, in the presence of an initiator and a cross-linker [3, 7]. PCM has a wide range of applications involving ophthalmic operations [8], drug treatment [9], and food packaging [10]. In the field of water purification, PCM has proved itself as an efficient adsorbent for water pollutants since it is a stable, elastic, stretchable, nonionic, non-resorbable, low-cost watery gel. Also, it has a pH-independent swelling behavior, recoverability, and a high adsorption capacity [3, 11, 12]. It is composed of ~ 2.5% cross-linked polymer, rich in amide functional groups and water, depending on the concentration of monomer [3]. It is worth mentioning that PCM is adaptable for drinking water treatment in many countries [12]. Due to its interesting structure-properties relationship, PCM can be used as a promising adsorbent for contest and carcinogenic dyes through abundant active sites that are capable of fixing dye molecules [11]. Moreover, it does not need a lot of expenses including energy, effort, or

*Corresponding author e-mail: a7mdghanem@gmail.com (Ahmed F. Ghanem)

Receive Date: 16 September 2024, Revise Date: 14 October 2024, Accept Date: 16 October 2024

DOI: 10.21608/ejchem.2024.321233.10436

time to be separated at the end of the adsorption course. However, polyacrylamide has some boundaries as it requires careful dosage control, mechanical degradation related to mixing speed, settling time to achieve the best optimal treatment performance, limited reaction rate at the beginning of the adsorption process, and restricted reusability [13]. Moreover, its adsorption capacity has to be enhanced to uptake more pollutant molecules [14]. On the other hand, PCM may cause health problems because, under certain conditions, toxic acrylamide monomer can be leaked leaving the polymeric matrix and causing toxicity of water [15]. In order to overcome its limitations and enhance its performance, people modified PCM with different approaches such as copolymerization, doping, blending, and compositing [16-20].

Indeed, several articles have been released discussing the possible inclusion of zeolite crystals in the polyacrylamide hydrogel [21-27]. However, the published articles were varied not only in the methods of preparations but also in the source of zeolites and their applications. Particularly, zeolite materials have been paid strong attention due to their unique properties in terms of high surface area, natural abundance or ease of being synthesized in many sizes, safety, and cost-effectiveness. Generally, zeolite structure comprises aluminum oxide and silicon silicates linked together by oxygen atoms at the corner of formed tetrahedral aluminosilicates three-dimensional crystal [28]. This distinctive crystal structure enjoys interconnected pores and tunnels of different sizes giving zeolite the ability to uptake pollutants in a gas or a liquid state not only on its surface but also inside its cavities [29]. Therefore, zeolite groups have found strong workability in water treatment applications as they are usually called molecular sieves [30, 31]. No doubt, the inclusion of zeolite particles as adsorptive filler to the polymer matrix could provide synergistic effects concerning the performance, the improvement of physicochemical properties, the better dispersion for zeolite particles, and hence avoiding the frequent aggregation and coagulation of zeolite itself while varying the conditions [21].

Accordingly, this work aimed to develop a polyacrylamide hydrogel incorporated with sodium zeolite particles obtained from Egyptian kaolin to be evaluated as an adsorbent for dye in wastewater. In this study, the composite hydrogel was prepared via in-situ polymerization of acrylamide monomer in the presence of different zeolite ratios. Then, the obtained modified hydrogels were investigated against the adsorption of methylene blue in synthetic wastewater. The highest-performance composite hydrogel was characterized by several physical techniques such as scanning electron microscope, X-ray diffraction, N_2 sorption, and Fourier transform infrared. Moreover, the reaction conditions in terms of the contact time, the adsorbent weight, the initial concentration, pH, and the temperature were optimized. Kinetic studies, adsorption models, and thermodynamics parameters were intensively discussed to understand the behavior and describe the performance of the suggested adsorbent towards the removal of dye. To the best of our knowledge, this assessment has not been investigated previously in the literature utilizing this proposed composite hydrogel given the opportunity for a new class of dye adsorbents.

2. Experimental

2.1. Materials

Acrylamide monomer (ACM, 99%) and N, N` methylene bis acrylamide (NBA) were supplied from ALPHA CHEMIKA, India. Potassium per sulphate (KPS, 99.99 %) was bought from Sigma-Aldrich, USA. Egyptian kaolin was provided from a kaolin factory located in Saint-Katerine, Sinai Peninsula, Egypt. The collected kaolin was well-washed with deionized water and calcinated at 450 ^oC for 4 hrs. before use. Methylene blue (MB) was supplied from Fluka Chemie GmbH (Germany).

2.2. Preparation of Polyacrylamide Hydrogel (PCM)

In the typical method, acrylamide, as a commercial precursor, was dissolved in the distilled water to form a homogenous solution of 12 % monomer concentration. Then, 0.2 % of NBA, as a common crosslinker, was added directly to the prepared solution and the temperature was raised to 60 ^oC. After 20 min., 0.2% KPS, as an initiator for the polymerization reaction, was dropped slowly under vigorous stirring. The reaction mixture was left at the previous conditions till the polyacrylamide hydrogel was formed. Finally, the reaction vessel was left to cool on a stand (Scheme 1). Then, the hydrogel was collected and kept in a plastic package in the fridge environment for further usage and characterization.

2.3. Preparation of Sodium Zeolite Particles (SZP)

A certain weight of the calcinated kaolin was aged in a strong sodium hydroxide solution. After 24 hrs., the mixture was transferred to a Teflon tube positioned in a sealed autoclave. Then, the system was transferred into the oven at 100 ^oC. After 9 hrs., the autoclave was kept under cooling overnight followed by washing of the product several times till normal pH. Finally, the produced zeolite powder was collected and dried at 80 ^oC for 24 hrs. (Scheme 1).

2.4. Preparation of Zeolitic Polyacrylamide Hydrogel (ZCM)

The composite was prepared via an in-situ polymerization approach. In this experiment, a fixed percentage of the prepared zeolite was well-dispersed in the distilled water overnight. Then, acrylamide (12 %) and NBA (0.2%) were added directly and the temperature was raised to 60 ^oC. After 20 min., KPS (0.2%) was dropped slowly under vigorous stirring to initiate the polymerization reaction. The composite polyacrylamide hydrogel was formed after a few minutes. Finally, the obtained product was left to cool on a stand and then preserved in a plastic package in the fridge environment (Scheme 1). Different concentrations of filler were added at the same conditions to prepare composite hydrogel with 5, 10, 20, 50, and 70 % zeolite particles.

2.5. Techniques

The morphology of the prepared zeolite in addition to polyacrylamide hydrogel before and after the modification process was investigated using a scanning electron microscope (JEOL-SEM with an acceleration voltage of 80 kV, USA). The nature of the interaction

between the synthesized hydrogel and the zeolite particles along with the alteration in the crystal structure were discussed with Fourier transform infrared (JASCO 4600, USA) and X-ray diffraction (Bruker D 8 advance target, USA), respectively. Finally, the surface texture in terms of BET surface area and the total pore volume were determined with the nitrogen gas sorption apparatus (Quantochrome Nova-Touch 4LX, USA).

2.6 Adsorption Batch

In this study, methylene blue was used as a model cationic dye in order to investigate the ability of the prepared hydrogels to decolorize the synthetic dye solution. In this experiment, a certain weight of the hydrogel (as undried gel) was taken in 50 mL of MB solution of a certain concentration. The flask was then shaken in a water bath (DAIHAN Scientific Bath) at a fixed temperature and 110 rpm over a while from 2 to 30 minutes. The remained dye after the adsorption was determined by UV-vis spectrometer (JASCO-V730). During this investigation, the influencing factors including the effects of pH, adsorbent weight, initial dye concentration, and reaction temperature were optimized against the contact time.

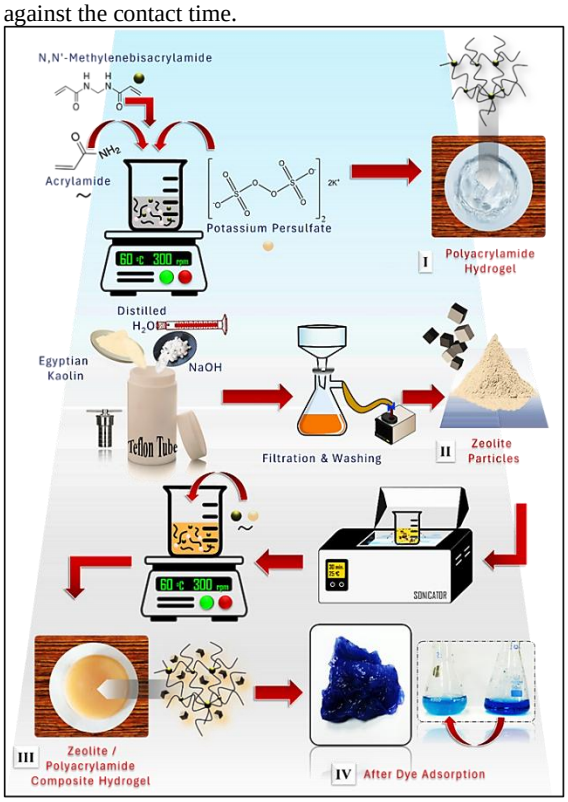

Scheme 1: Experimental representation for [I] Synthesis of pure polyacrylamide hydrogel (PCM), [II] Synthesis of zeolite particles (SZP), [III] Inclusion of zeolite particles in polyacrylamide matrix (ZCM), and [IV] Adsorption of methylene blue on the prepared composite hydrogel.

3. Results and Discussions

3.1. Microscopic Analysis

The morphology of the prepared zeolite, polyacrylamide hydrogel, and their composite was investigated with a scanning electron microscope and energy-dispersive X-ray spectroscopy. Figure 1[A] depicts the cubic particles characteristic of the morphology of sodium A zeolite in accordance with previous articles [32, 33]. The zeolite particles were obtained in the range between 400 to 800 nm with an average size of 600 nm, Fig. 1[E]. Figure 1[B] showed an unusual surface structure of polyacrylamide as the common porosity of the hydrogel [34] did not appear despite the relativity rough surface. This might be attributed to the drying step in the oven. Drying might cause pores to collapse as a result of heat under a vacuum. Other studies recorded the same observed morphology for the polyacrylamide hydrogel [35-37]. The incorporation of zeolite particles displayed well distribution in the PCM matrix, Fig. 1[C], despite some aggregations of cubic zeolite particles (red arrows) on the surface were also seen, Fig. 1[D]. EDX confirmed the successful inclusion of zeolite crystals in the hydrogel matrix as shown in Fig. 1[F]. However, the spectrum presented low-intensity peaks with low atomic percentages assigned to sulfur and potassium atoms. This reveals the residues of the initiator used for the polymerization reaction; potassium persulphate.

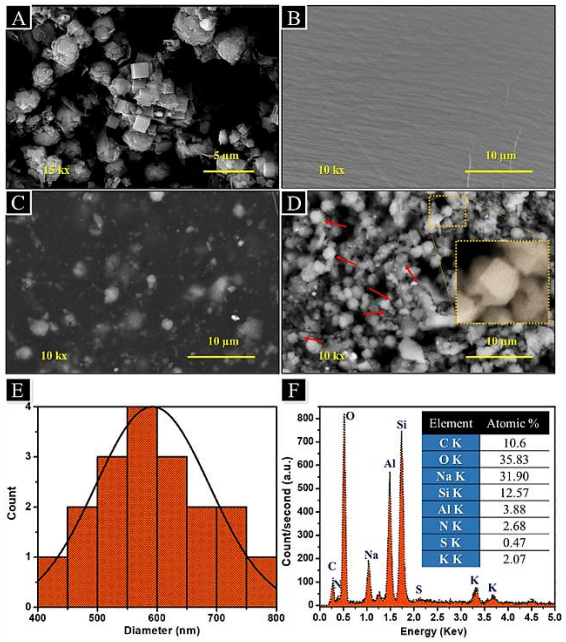

Figure 1: SEM micrographs for pure Na-A zeolite particles (SZP) [A], pristine polyacrylamide hydrogel (PCM) [B], and their composite (ZCM, 10 *wt.*% zeolite) at different sceneries [C-D]. [E] Particle size distribution for zeolite particles, and [F] EDX spectrum for the prepared composite hydrogel.

3.2. X-ray Diffraction

The crystalline structure of the obtained sodium zeolite was confirmed with XRD as depicted in Fig. 2. Obviously, the characteristic lines of zeolite appeared at 2θ ~ 7°, ~10°, ~12.3°, ~16°, ~24°, ~30°, ~36.5°, ~39°, ~43°, and ~50° corresponding to (200), (220), (222), (420), (622), (644), (1000), (1042), (880), and (1082) reflection planes, respectively, in accordance with (JCPDS card no. 390-222) and state of art [38]. According to previous reports, polyacrylamide has

an amorphous structure [39]. However, the inclusion of zeolite crystals in the polyacrylamide matrix improved its crystallinity. Moreover, the main XRD peaks of zeolite are pronounced clearly in the composite gel (ZCM) spectrum in their positions without a significant shift. Some other peaks were embedded under the broad band of polyacrylamide. These results confirmed the successful synthesis of the hybrid gel in which zeolite particles physically interacted with the polymer matrix. Faghihian and his colleague acquired the same observation when β-zeolite / polyacrylamide / phytic acid composite was prepared [23].

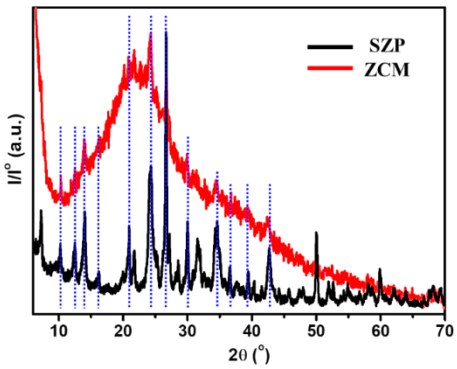

Figure 2: XRD spectra for the prepared sodium zeolite particles (SZP) and composite poly-acrylamide hydrogel (ZCM, 10 wt.% zeolite)

3.3. Fourier Transform Infrared (FTIR)

The successful preparation of polyacrylamide and zeolite particles in addition to the nature of interaction between them in the obtained composite hydrogel was verified with FTIR as shown in Fig. 3[Left]. Particularly, the spectra demonstrate several functional groups present on the surface of prepared substances. Polyacrylamide hydrogel showed characteristic peaks at (~ 3400 - ~3200), ~ 2920, ~ 1621, ~ 1380, and (~1089 - ~ 1047) cm^{-1} corresponding to asymmetric stretching vibrations of amino groups, alkyl, deformation of NH_2, -C-N, and twisting of NH_2, respectively. These values are close to the previous reports [40, 41]. However, the band of -C=O of the amide group was not observed at ~ 1650 cm^{-1} which might be overlapped with the near band of -NH_2 deformation. Sodium zeolite displayed main bands at ~ 3300, ~ 1660, ~ 970, ~ 804, and ~ 532 cm^{-1} assigned to starching vibration of -OH, bending vibration of sorbed water, asymmetric stretching vibration of Si-O-Si, stretching vibration of Al–O, and its bending vibration, respectively, following the state of art [42].

For the first look at the spectrum of composite hydrogel, all the bands appeared identical without a significant shifting even after the inclusion of zeolite particles in the polyacrylamide hydrogel. However, by scaling in and a careful inspection of the spectrum, one can observe a slight shift in some peaks i.e. 3470 to 3465 cm^{-1}, 3546 to 3542 cm^{-1}, 3236 to 3240 cm^{-1}, 856 to 854 cm^{-1}, and other shifts in the fingerprint region. Moreover, increasing the intensities of some peaks and decreasing others along with the disappearance of zeolite bands were perceived in the composite spectrum. Indeed, several reports discussed the possible interactions between the clay and the polyacrylamide matrix, during in-situ polymerization which is similar to the used approach in the present study, with the same significant alterations in the spectra [43-45]. Briefly, the disappearance of Si-O-Si might be due to the possible hydrolysis in the solution and the formation of a silanol group (Si-OH). This functional group could interact through a hydrogen bonding with the amide group. Another suggested mechanism presumed a physical interaction can be established, depending on the solution pH, between the ionized silanol groups and the partially positively charged hydrogen atoms of the amide groups [45]. Thus, it could be claimed that the slight shifting observed in the polymeric spectrum and the absence of zeolite bands might be attributed to the hydrogen bonding arising between the amide groups and the zeolite hydroxyl groups. This emphasized the successful assembly of the polymer network around the zeolitic particles in the crosslinked hydrogel, Fig. 3[Right].

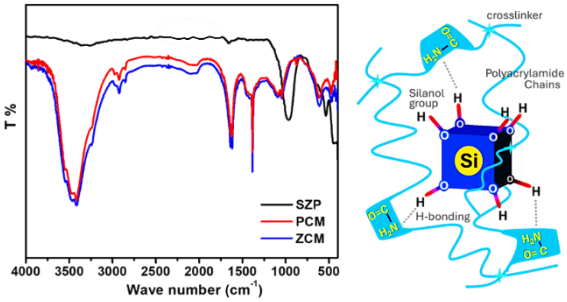

Figure 3: [Left] FTIR spectra for the prepared sodium zeolite particles (SZP), polyacrylamide hydrogel (PCM), and their composite hydrogel (ZCM, 10 wt.% zeolite). [Right] Schematic representation for the possible interaction between the zeolite particles and the crosslinked polyacrylamide hydrogel

3.4. Surface Texture

Figure 4 depicts N_2 adsorption/desorption isotherms for the prepared polyacrylamide and its composite. The curves showed that the samples have IV type of isotherm with H3 type of hysteresis loop, attributed to the capillary condensation, Fig. 4[Left].

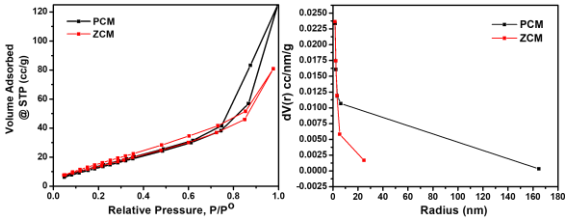

Figure 4: [Left] N_2 adsorption/desorption isotherms of polyacrylamide hydrogel (PCM) and its zeolite composite (ZCM, 10 *wt.*% zeolite). [Right] The corresponding pore size distribution plot determined by BJH- method

However, the composite hydrogel showed a lower hysteresis. Moreover, the inclusion of zeolite particles caused a significant alteration in the pore radius as

presented by BJH pore size distribution, Fig. 4 [Right]. It could be claimed that the prepared composite hydrogel is characterized by a mesoporous structure thanks to zeolite particles that could be used as a mesoporous agent for the polymeric matrices [33, 46]. On the other hand, the presence of zeolite particles displayed a slight increment in the surface area with a slight decrease in the total pore volume, Table 1. As can be expected, the adsorption behavior of the modified polyacrylamide would be improved as will be illustrated later on.

Table 1: Textural properties of the polyacrylamide hydrogel (PCM), and its composite (ZCM, 10 *wt.*% zeolite)

Textural Parameters	PCM	ZCM
Multipoint BET surface area (m^2/g)	59.76	61.35
Correlation coefficient (R^2)	0.967	0.998
Langmuir method (m^2/g)	118.012	108.82
Adsorption BJH surface area (m^2/g)	48.623	44.64
Adsorption BJH cumulative micropore volume (cc/g)	0.188	0.116
Pore radius BJH adsorption (nm)	1.703	1.686
Total pore volume (cc/g)	0.193	0.125
Average pore radius (nm)	6.487	4.087
Average Particle radius (nm)	2.281	6.041

3.5. Dye Adsorption

The Effect of zeolite percentage in the polyacrylamide matrix was studied at an initial dye concentration of 50 ppm, normal pH, and adsorbent weight (3 g) of hydrogel (used as prepared without drying) at 28ºC. The ratio of zeolite particles was changed from 5 to 75 *wt.* % (according to monomer weight). Figure 5[A] indicates that the highest removal percentage, ~ 82 % after only two minutes of treatment, was recorded by the sample containing 10 *wt.*% compared with the unmodified hydrogel. Increasing the loading ratio did not present a higher removal attributed to the possible aggregation in the gel matrix. Therefore, the sample includes 10 *wt.* % was selected for further experiments. Moreover, it can be noticed that the rate at the beginning of the reaction increased thanks to the presence of zeolite particles.

Figure 5[B] represents the effect of pH media, in the range from 2 to 10, on the removal of MB utilizing the modified hydrogel. As shown, the dye uptake mostly was not strongly influenced by the changes in the pH of the medium. However, polyacrylamide hydrogel was found to remove MB at high pH [14]. Particularly, in the present case, MB can be eliminated by the prepared composite hydrogel at normal pH which is favourable from the economic and the environmental point of view. Thus, all the next experiments would be performed at the normal pH (7.5).

The adsorbent dose of the undried hydrogel was investigated starting from 0.5 g up to 5 g and the MB removal was recorded, Fig. 5[C]. Obviously, increasing the gel's weight led to an increase in the dye uptake thanks to the located active adsorption sites and the enhanced surface area (c.f. Table 1) [47]. However, no improvement between 3 g and 5 g can be considered. Thus, the adsorbent mass was set at 3 g for the further trails.

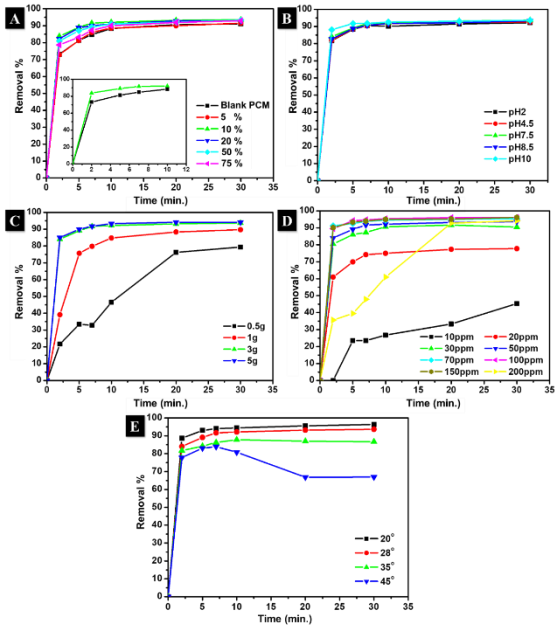

Figure 5: [A] Effect of zeolite concentration in polyacrylamide matrix compared with pristine (Initial dye concentration: 50 ppm, normal pH, adsorbent weight: 0.4g dried gel, volume: 50mL, and 28º). [B] Effect of pH at initial concentration: 50 ppm, zeolite in polyacrylamide: 10 *wt.*%, adsorbent weight: 0.4g dried gel, volume: 50mL, and 28º). [C] Effect of adsorbent weight at initial concentration: 50 ppm, normal pH, zeolite in polyacrylamide: 10 *wt.*%, adsorbent weight: 0.4g dried gel, volume: 50mL, and 28º. [D] Effect of initial dye concentration at normal pH, zeolite in polyacrylamide: 10 *wt.*%, adsorbent weight: 0.4g dried gel, volume: 50mL, and 28º. [E] Effect of the reaction temperature at initial concentration: 100 ppm, normal pH, zeolite in polyacrylamide: 10 *wt.*%, adsorbent weight: 0.4g dried gel, and volume: 50mL. All optimized factors were studied against contact time.

No doubt, studying sorbate concentration is crucial to understand the behaviour of the used adsorbent. Particularly, the initial dye concentration was varied from 10 to 200 ppm and the dye uptake was determined, Fig. 5[D]. It was observed that the amount of MB adsorbed was large at the first two minutes i.e. the reaction rate was rapid. Then, the rate tended to be slower for a prolonged time till finally reached saturation. Besides, the composite hydrogel showed relatively uncommon behaviour. As shown, the removal percentages were found to increase by increasing the initial dye concentrations. Moreover, at higher concentrations (50 - 150 ppm), the adsorption was highly competitive to achieve the highest removal i.e. the removal percentage increased from 93.68 to 96.12 %. MB molecules will probably diffuse more readily from the fluid phase to the adsorbent surface at higher dye concentrations [48]. The same observation was recorded

by Badawy et. al. [49]. As stated also in another study, the high adsorption might be revealed to the elevated mass transfer of dye molecules towards the surface [50]. However, at 200 ppm, it was observed that the removal was slower till reached the highest percentage (~ 93.4 %) after 20 minutes. This might be attributed to the saturation of the surface-active sites. It could be claimed that the proposed composite hydrogel discussed in this work can extract a greater quantity of MB from the aqueous solution within a few minutes. This is significant for the potential uses as adsorbents for the removal of cationic pollutants from wastewater.

The adsorption reaction was also checked at different temperatures starting from 20° up to 45° at an initial dye concentration of 50 ppm, Fig. 5[E]. As depicted, by increasing the reaction temperature, the adsorption decreased as the highest removal percentage was recorded at 20°. This emphasizes that the reaction is exothermic. Different parameters were calculated to confirm this observation would be illustrated later on.

According to the aforementioned discussions, the optimized conditions for MB adsorption over the prepared composite hydrogel were zeolite ratio: 10 *wt.* %, normal pH, adsorbent weight: 3 g (undried gel) or 0.4 g (dried gel) / 50 mL, initial dye concentration: 150 ppm, and reaction temperature: 20 °C.

3.6. Adsorption Isotherm

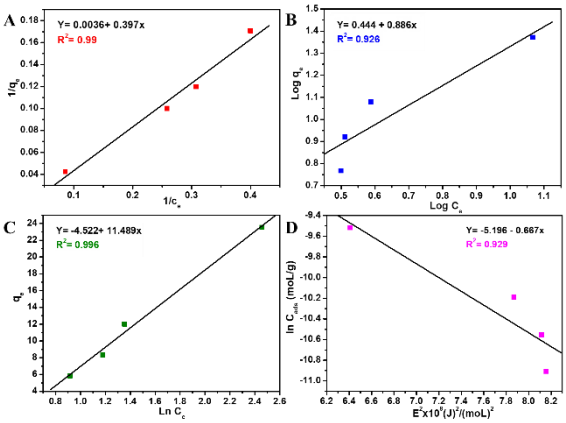

Figure 6: [A] Langmuir, [B] Freundlich, [C] Temkin, and [D] Dubinin sorption isotherms of methylene blue on the composite hydrogel (ZCM, 10 *wt.*% zeolite).

In order to understand the adsorption process, in this study, four common models for analysing equilibrium adsorption data were intensively investigated. Figure 6[A] presents the Langmuir adsorption model, a popular adsorption model, assuming that the adsorption solely can take place on the surface of the adsorbent. This allows the model to explain experimental data throughout a wide concentration range. The mathematical expression for this model is shown in Eq. 1.

$$\frac{1}{q_e} = \frac{1}{K_L\ q_{max}} \cdot \frac{1}{C_e} + \frac{1}{q_{max}} \qquad (1)$$

The parameters in Langmuir's equation designate the adsorption capacity (qe), equilibrium concentration (Ce), maximum adsorption capacity (q_{max}) in mg/g, and Langmuir's constant (K_L) in L/mg. Particularly, K_L explains the binding affinity between the sorbate and the adsorbent. It can be also determined using another term (R_L), commonly known as the separation factor, which can be expressed in Eq. 2.

$$R_L = \frac{1}{1+C_i\ K_L} \qquad (2)$$

Generally, R_L has several values that can provide more information about the adsorption. When R_L equals zero, this means that the adsorption reaction is irreversible. Linear adsorption can be obtained when R_L equals unit. However, favourable or unfavourable adsorption becomes identified when $0 < R_L < 1$ or $R_L > 1$, respectively. Table 2 summarises Langmuir's parameters in terms of maximum adsorption capacity, Langmuir constant, and separation factor. Additionally, Table 3 presents reported adsorbents of different q_{max} compared with the present study. As shown, the prepared composite hydrogel exhibits a superior value confirming its highest workability.

Figure 6[B] shows the Freundlich model which reveals that multilayer adsorption can take place at irregularly distributed adsorption sites. Equation 3 expresses this model.

$$q_e = K_f\ C_e^{1/n} \qquad (3)$$

where, n and K_f represent the adsorption speed and the adsorption capability constants, respectively, in mg/g. Specifically, values closer to or equal to 1 indicate a material with generally homogeneous binding sites. However, 1/n, the heterogeneity factor, indicates a heterogeneous adsorbent. Also, Table 2 lists the Freundlich parameters. Accordingly, from Fig. 6[A-B], the adsorption obeys the Langmuir model as R^2 was found higher than that determined by Freundlich. Therefore, the maximum adsorption capacity was calculated and found to equal 275 mg/g. It is worth mentioning that, polyacrylamide was previously investigated against MB removal and the adsorption capacity was found 111 mg/g at optimum conditions of pH 8, 25°, and 120 min. [14].

The adsorbent-adsorbate interaction was taken into account by the Temkin isotherm, Fig. 6[C]. Mainly, the model assumes that the heat of adsorption (function of temperature) of all molecules in the layer would decrease linearly rather than logarithmic with coverage [51]. Temkin model's parameters can be given by Eq. 4.

$$q_e = B\ \ln A_T + B\ \ln C_e \qquad (4)$$

T, R, A_T, B, and q_e assign the absolute temperature, the universal gas constant (8.314 J/mol K), the equilibrium binding constant (L/mg), the constant related to the heat of adsorption (J/mol), and the amount of adsorbate adsorbed at equilibrium (mg/g), respectively. B can be also obtained B= RT/b. Plotting q_e against ln Ce gives a straight-line curve. From the slope (B) and the intercept (A_T) can be determined. The results indicate the positive value of B (11.489 J/mol) confirming that the adsorption is exothermic. Moreover, A_T was found to equal 0.674 L/mg related to the high affinity of MB molecules to ZCM. This observation was also confirmed by thermodynamics studies as would be illustrated later on.

Dubinin-Radushkevich isotherm is usually utilized in order to clarify the mode of adsorption either chemical or

physical interaction. Dubinin model provides mathematical relations in Eq. (5-7).

$$q_e = q_{max} \exp(-K \varepsilon^2) \quad (5)$$

$$\varepsilon = RT [1 + 1/C_e] \quad (6)$$

The amount of adsorbate adsorbed at equilibrium is denoted by qe, maximal adsorption capacity qmax, R is the gas constant, B is the Dubinin-Radushkevich constant, T is absolute temperature, and Ce is the adsorbate's equilibrium concentration. Consequently, a straight-line plot was given. The slope identifies term B and the intercept of ln qmax will result from plotting lnqe versus ε^2. Additionally, the free energy of sorption per molecule of the adsorbate, E, can be calculated from the value of B using Eq. 7.

$$E = 1/\sqrt{2B} \quad (7)$$

The energy of adsorption (E) illustrates the kind of adsorption taking place. When the value of E becomes between 1 - 8 kJ/mol, this confirms the physical adsorption. Meanwhile, values between 8 and 16 kJ/mol emphasize the chemical adsorption [52]. Since the value of free energy was found to equal 8.65 kJ/mol, it indicated that the chemisorption interaction played a significant role in the adsorption of MB over ZCM.

3.7. Kinetics Studies

Adsorption kinetics were studied and depicted in Fig. 7. Also, Table 2 displays the pseudo-first and the pseudo-second-order kinetic parameter values for MB adsorption over the prepared composite hydrogel. The best kinetic adsorption model was determined by applying the correlation coefficient criterion, which is defined as the maximum value of R^2 [53].

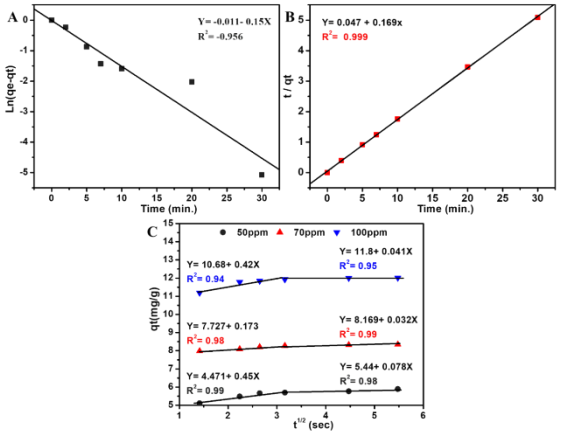

Figure 7: [A] First-order kinetic model, [B] Second-order kinetic model, and [C] Intra-particle diffusion model for the adsorption of MB over the composite hydrogel (ZCM, 10 wt.% zeolite)

As shown, the R^2 value was found more than 0.99, for the adsorption under investigation, according to the pseudo-second-order (PSO) kinetic model. Particularly, this mathematical model proved the chemical adsorption between the adsorbent and the adsorbate in the form of ionic interaction. Weber-Morris model showed that the plot of qt vs. $t^{0.5}$ will pass through the origin in case the intraparticle diffusion (IPD) is the rate-controlling factor. However, IPD deviation from the origin proposes that two processes had occurred and the IPD is not the only rate-determining step [54]. The IPD plot shown in Fig. 7[C] has two separate linear sections that strengthen the involvement of other mechanisms such as the film diffusion mechanism. Additionally, the lower C1 compared to C2 in IPD suggested a faster process during the first stage of adsorption, and both increased as C0 increased, indicating a concentration-dependent process [55]. However, the adsorbate structure and its related functional groups, the textural characteristics of the adsorbents, and the nature of the adsorbate–adsorbent interaction are generally important elements that can influence the adsorption process in addition to the diffusion process [56].

Table 2: Isothermal, kinetic, and thermodynamic parameters for the adsorption of MB over ZCM

Parameters		Langmuir Model
q_{max}(mg/g)		274.72
K_L(L/mg)		0.0091
R_L		0.686
R^2		0.99
		Freundlich Model
1/n		0.848
K_f		2.779
R^2		0.96
		Temkin Model
Bt(J/mol)		11.489
A_T(L/mg)		0.674
R^2		0.99
		Pseudo-First-Order
qe, calc.		0.988
K1		-0.005
R^2		-0.95
		Pseudo-Second-Order
qe, calc.		5.917
qe, exp.		5.893
K2		0.607
R^2		0.999
		Intraparticle Diffusion
K_{1diff}	at 50ppm	0.45
K_{2diff}		0.078
C_{1diff}		4.471
C_{2diff}		5.444
R^2		0.999
		ΔG (kj/mol)
Temp. (°C)	20	-2.93358
	28	-1.21095
	35	0.523838
	45	3.63362
ΔH (kj/mol)		-88.47
ΔS (J/mol·K)		-292.98

3.8. Adsorption Thermodynamics

The thermodynamics were studied at different temperatures and $\ln K_L$ vs. 1/T was plotted, Fig. 8. According to the results presented in Table 2, the adsorption process is spontaneous and favoured at low temperatures (20 and 28^{0}C) as the Gibbs free energy

(ΔG°) had a negative value [57]. However, at higher temperatures, the values of Gibbs free energy were found positive implying that the adsorption process is not spontaneous or even favourable. Additionally, the standard enthalpy for the used substrate was negative (ΔH°=-88.47 kJ.mol^{-1}), indicating the exothermic reaction. Moreover, this elaborates that the adsorption was not constrained by the diffusional step only and there are strong interactions between the adsorbate and the adsorbent. The adsorption mechanism, which involves the transition from a random state (dye in solution) to a more ordered one (dye interacting with the substrate), was well supported by the negative sign of ΔS° [58].

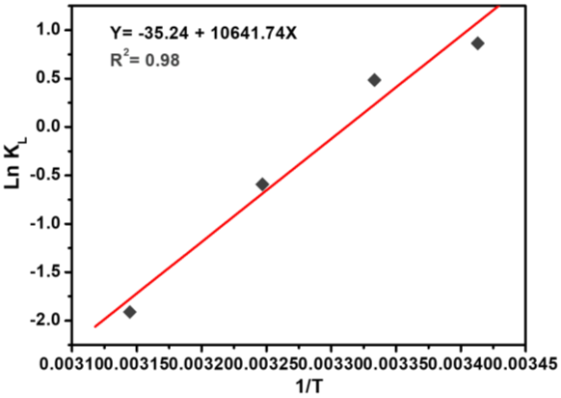

Figure 8: Thermodynamic curve for methylene blue adsorption

Table 3: Comparison between the reported adsorbents and the prepared composite hydrogel (ZCM) in terms of adsorption capacity

Adsorbent Type	q_{max} (mg/g)	Reference
Polyacrylamide (PAA) hydrogel	111.1	[14]
Chitosan cross-linked with zeolite	242.51	[53]
Hierarchical zeolite (MY)	133.1	[54]
PBAT-Z-6M mat	100	[55]
CMC/CNC/zeolite/citric acid	38.2	[56]
PAM/GO hydrogel	255.48	[57]
Polyvinyl alcohol /carboxymethyl cellulose	172.14	[58]
PAM/Zeolite composite hydrogel	274.72	This study

3.9 Adsorption Mechanism

FTIR tool was used in order to confirm the successful adsorption of MB over the composite hydrogel. As revealed in Fig. 9 [Top], the two spectra demonstrate the chemical structures of ZCM before and after the adsorption of dye. Mostly, the bands are identical and overlapped with an obvious decrease in the gel peaks' intensities. However, some peaks were found shifted particularly in the region of -NH_2 twisting (c.f. Fig.3). According to the state of art, both components of composite hydrogel have the ability to remove MB in different ways. Particularly, Prajaputra et.al stated that zeolite is negatively charged permanently thanks to the isomorphic substitution of Si^{4+} with Al^{3+} in its structure.

These charges could ionically interact with cationic dye forming polyion complexes due to the opposite charges of both molecules [65].

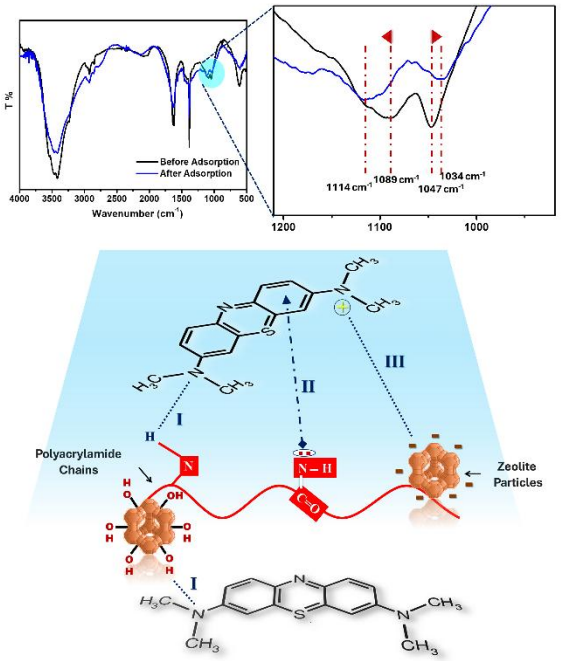

Figure 9: [Top] FTIR of the composite hydrogel before and after MB adsorption. [Bottom] Schematic representation for the proposed adsorption mechanism (I, II, and III donate to hydrogen bonding, n-π sharing, and ionic interaction, respectively).

Additionally, as previously discussed in section 3.3, surface hydroxyl groups can be created on the surface of zeolite which also can contribute to the interaction with the dye molecules through hydrogen bonding [66]. On the other hand, polyacrylamide hydrogel backbone can interact with the dye structure through two bonds. Amide groups can form hydrogen bonding with nitrogen groups of dye. Alternatively, n–π interaction can be formed between the –NH group (as an electron donor group carrying pairs of electrons on the oxygen atom) and the phenyl rings of MB (as acceptors) similar to the previous report [67]. The proposed mechanism of methylene blue adsorption over the composite hydrogel is represented in Fig. 9. No doubt, these investigations emphasized the strong plausible interactions in agreement with the findings of thermodynamic and adsorption models.

3.10. Reusability

One of the most features of adsorbent is the reusing capability. Most efficient adsorbing materials have to be used frequent times to remove the same pollutants keeping their performance high. In the present study, the prepared composite hydrogel was reused up to five times. However, the selection of the washing solvent and optimizing washing conditions strongly affected the performance of adsorbent in the successive cycles. Particularly, ethanol can be used as an extractor for dye from the surface of adsorbent [59, 60]. Four experiments

were carried out in order to determine the best ethanol concentration should be used to detach dye molecules from the surface of composite hydrogel after the course of treatment keeping other conditions fixed. The concentration was selected according to the ability to remove MB in the first run i.e. the first cycle for the adsorbent after washing with ethanol. Figure 10[Top] indicates that using 100% ethanol was the best concentration to remove MB and achieved the highest removal % in the first run. Meanwhile, using diluted ethanol (25%) showed the lowest uptake.

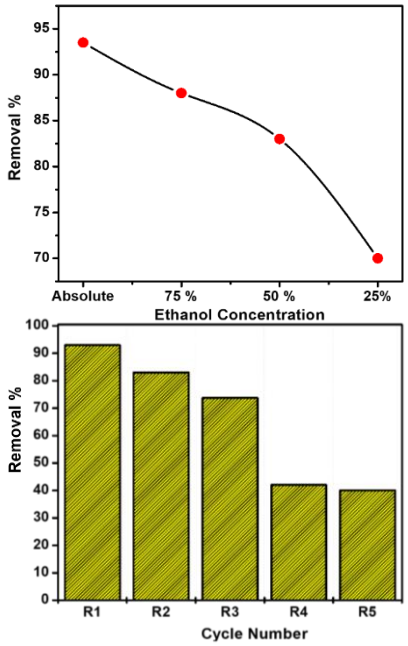

Figure 10: [Top] The removal percentage of MB after the first run only using different concentrations of ethanol as a dye extractor (washing time: 15 minutes, volume: 50 mL, and RPM: 150). [Bottom] Reusability of ZCM against the removal of MB up to five cycles

This reveals the strong workability of ethanol to clean the adsorbent surface from MB. This might be also more feasible and favorable in water treatment applications as using the treated water to wash the adsorbent does not make sense. Additionally, by evaporating ethanol, the dye can be recovered once again i.e. circular economy. It is worth mentioning that, the time consumed for the washing process with absolute ethanol was only 15 minutes and no significant improvement was detected by prolonged washing time. Accordingly, absolute ethanol was selected to clean the composite hydrogel in all successive cycles. As shown in Fig. 10[Bottom], the composite hydrogel can be used up to five rounds. However, the removal % decreased slowly from 93 till reached 40 after the fifth cycle. This might be attributed to the inability of ethanol to detach the chemically adsorbed dye molecules from the surface as the thermodynamic and adsorption models refer to the existence of a chemical interaction between the MB molecules and the composite hydrogel's surface, which absolutely blocks the active sites and hence reduces the adsorbent efficiency.

4. Conclusions

In the present study, Na-A zeolite particles were obtained hydrothermally from Egyptian kaolin via a simple alkaline treatment. Then, the produced particles were used as a filler for the polyacrylamide hydrogel with different ratios. Generally, the composite hydrogel was prepared by prior dispersion of sodium zeolite particles in the acrylamide monomer solution followed by polymerization in the presence of KPS and NBA. SEM/EDX confirmed the successful synthesis of Na-A zeolite particles and their distribution in the polyacrylamide matrix. FTIR emphasized the hydrolysis of silane groups of zeolite into silanol groups that strongly interact with the amide groups on the surface of polyacrylamide through hydrogen bonding. XRD showed improvement in polymer crystallinity in the presence of zeolite particles. Nitrogen sorption results displayed increasing in the surface area and the mesoporosity of the prepared composite thanks to the mesoporous zeolite filler. This improved the removal of MB in the synthetic wastewater compared with the unmodified polyacrylamide hydrogel as the adsorption capacity increased up to ~ 275 mg/g. Optimization of the reaction conditions demonstrated the highest dye uptake (~96%) of 150 ppm/50 mL achieved after only five minutes using 0.4 g of dried composite hydrogel (10 *wt.*% zeolite) at normal pH, and 20 ^{o}C. Adsorption isotherms showed the highest R^2 of the Langmuir model. Meanwhile, the Temkin model confirmed the high affinity of MB molecules towards ZCM and the reaction is exothermic in agreement with the thermodynamic studies as well. Also, Dubinin model confirmed that a chemical reaction was established. Kinetic studies accentuated that the adsorption reaction is pseudo-second order. Reusability informed the feasibility of the prepared composite hydrogel to be used for five rounds utilizing absolute ethanol as a dye extractor from the adsorbent's surface.

5. Conflicts of interest

The authors declare there is no conflict of interest.

6. Acknowledgment

The authors gratefully thank the National Research Centre for the financial support of the in-house project no. 13010307 and PhD thesis no. 22/1/8.

7. References

1. Sinha, V. and S. Chakma, Advances in the preparation of hydrogel for wastewater treatment: A concise review. Journal of Environmental Chemical Engineering, 2019. 7(5): p. 103295.
2. Peppas, N.A. and A.G. Mikos, Preparation methods and structure of hydrogels, in Hydrogels in medicine and pharmacy. 2019, CRC press. p. 1-26.
3. Tangri, A., polyacrylamide-based hydrogels: synthesis, characterization and applications. International Journal of Pharmaceutical, Chemical & Biological Sciences, 2014. 4(4).
4. Badsha, M.A., et al., Role of surface functional groups of hydrogels in metal adsorption: From performance to mechanism. Journal of Hazardous Materials, 2021. 408: p. 124463.
5. Ali, N., et al., Nanoarchitectonics: Porous hydrogel as bio-sorbent for effective remediation of hazardous contaminants. Journal of Inorganic and

Organometallic Polymers and Materials, 2022. 32(9): p. 3301-3320.
6. Van Tran, V., D. Park, and Y.-C. Lee, Hydrogel applications for adsorption of contaminants in water and wastewater treatment. Environmental Science and Pollution Research, 2018. 25: p. 24569-24599.
7. Ali, R., et al., Synergistic Impact of Biochar Nanorods on the Performance of Polyacrylamide Matrix: UV-assisted Degradation of Phenol and Biological Activity. Egyptian Journal of Chemistry, 2024. 67(3): p. 431-448.
8. da Silva, A.L.B., et al., Intraorbital polyacrylamide gel injection for the treatment of anophthalmic enophthalmos. Ophthalmic Plastic & Reconstructive Surgery, 2008. 24(5): p. 367-371.
9. Sille, I.E., et al., Antimicrobial-loaded polyacrylamide hydrogels supported on titanium as reservoir for local drug delivery. Pathogens, 2023. 12(2): p. 202.
10. Rukmanikrishnan, B., S. Ramalingam, and J. Lee, Quaternary ammonium silane-reinforced agar/polyacrylamide composites for packaging applications. International Journal of Biological Macromolecules, 2021. 182: p. 1301-1309.
11. Lebkiri, I., et al., Swelling properties and basic dye adsorption studies of polyacrylamide hydrogel. Desalination and Water Treatment, 2021. 233: p. 361-376.
12. Bae, Y.-H., et al., Potable water treatment by polyacrylamide base flocculants, coupled with an inorganic coagulant. Environmental Engineering Research, 2007. 12(1): p. 21-29.
13. Ho, Y., et al., Enhanced turbidity removal in water treatment by using emerging vegetal biopolymer composite: a characterization and optimization study. Desalination and Water Treatment, 2016. 57(4): p. 1779-1789.
14. Mousavi, H.Z., et al., Application of polyacrylamide for methylene blue removal from aqueous solutions. Journal of Applied Solution Chemistry and Modeling, 2014. 3(1): p. 39-47.
15. Zhang, K., et al., Treatment of polyacrylamide production wastewater by multistage contact reactor with activated and anammox sludge. Biochemical Engineering Journal, 2019. 150: p. 107287.
16. Lin, X., et al., A multifunctional polyacrylamide/chitosan hydrogel for dyes adsorption and metal ions detection in water. International Journal of Biological Macromolecules, 2023. 246: p. 125613.
17. Ali, M.A.M., et al., Polyacrylamide hybrid nanocomposites hydrogels for efficient water treatment. Iranian Polymer Journal, 2020. 29: p. 455-466.
18. Zhu, X., et al., Graphene/polyacrylamide interpenetrating structure hydrogels for wastewater treatment. Advanced Composites and Hybrid Materials, 2023. 6(5): p. 169.
19. Song, X., et al., β-Cyclodextrin-Polyacrylamide hydrogel for removal of organic micropollutants from water. Molecules, 2021. 26(16): p. 5031.
20. Hamri, S., et al., Cleaning of wastewater using crosslinked poly (acrylamide-co-acrylic acid) hydrogels: Analysis of rotatable bonds, binding energy and hydrogen bonding. Gels, 2022. 8(3): p. 156.
21. Ulusoy, U. and S. Şimşek, Lead removal by polyacrylamide-bentonite and zeolite composites: Effect of phytic acid immobilization. Journal of hazardous materials, 2005. 127(1-3): p. 163-171.
22. Puspitasari, T., et al. Synthesis and characterization of zeolite-g-polyacrylamide (Zeolite-g-PAAM) by using simultaneous irradiation technique. in Journal of Physics: Conference Series. 2020. IOP Publishing.
23. Faghihian, H. and S.N. Farsani, Modification of polyacrylamide–β–zeolite composite by phytic acid for the removal of lead from aqueous solutions. Polish Journal of Chemical Technology, 2013. 15(1): p. 1-6.
24. Dabizha, O., T. Khamova, and O. Shilova, Mechanochemical Modification of Zeolite Rocks with Polyacrylamide for the Preparation of Oil Sorbents. Inorganic Materials, 2023. 59(10): p. 1127-1139.
25. Baybaş, D. and U. Ulusoy, Polyacrylamide–clinoptilolite/Y-zeolite composites: Characterization and adsorptive features for terbium. Journal of Hazardous Materials, 2011. 187(1-3): p. 241-249.
26. Wiśniewska, M., et al., Investigation of adsorption mechanism of phosphate (V) ions on the nanostructured Na-A zeolite surface modified with ionic polyacrylamide with regard to their removal from aqueous solution. Applied Nanoscience, 2020. 10: p. 4475-4485.
27. Abdulsada, Z.S., S.S. Hassan, and S.H. Awad, Removal of Some Heavy Metals from Polluted Water Using New Schiff Base for Polyacrylamide with Zeolite Nanocomposites. Baghdad Science Journal, 2024.
28. Moshoeshoe, M., M.S. Nadiye-Tabbiruka, and V. Obuseng, A review of the chemistry, structure, properties and applications of zeolites. Am. J. Mater. Sci, 2017. 7(5): p. 196-221.
29. Strzemiecka, B., et al., Examination of zeolites as fragrance carriers. Microporous and Mesoporous Materials, 2012. 161: p. 106-114.
30. Huang, Z., et al., Synthesis of 4A zeolite molecular sieves by modifying fly ash with water treatment residue to remove ammonia nitrogen from water. Sustainability, 2024. 16(13): p. 5683.
31. Liu, G., et al., Preparation of NaA zeolite molecular sieve based on solid waste fly ash by high-speed dispersion homogenization-assisted alkali fusion-hydrothermal method and its performance of ammonia-nitrogen adsorption. Journal of Science: Advanced Materials and Devices, 2024. 9(1): p. 100673.
32. Shoumkova, A. and V. Stoyanova, SEM–EDX and XRD characterization of zeolite NaA, synthesized from rice husk and aluminium scrap by different procedures for preparation of the

initial hydrogel. Journal of Porous Materials, 2013. 20: p. 249-255.
33. Ibrahim, S.M., et al., Effective single and contest carcinogenic dyes adsorption onto A-zeolite/bacterial cellulose composite membrane: Adsorption isotherms, kinetics, and thermodynamics. Journal of Environmental Chemical Engineering, 2022. 10(6): p. 108588.
34. Kim, S., et al., Polyacrylamide hydrogel properties for horticultural applications. International Journal of Polymer Analysis and Characterization, 2010. 15(5): p. 307-318.
35. Li, S., et al., Facile preparation of poly (acrylic acid–acrylamide) hydrogels by frontal polymerization and their use in removal of cationic dyes from aqueous solution. Desalination, 2011. 280(1-3): p. 95-102.
36. Musa, Y., et al., Polyacrylamide hydrogels for application in oral drug delivery. Nigerian Journal of Scientific Research, 2021. 20(4): p. 390-396.
37. Cha, H.-R., et al., Fabrication of amino acid based silver nanocomposite hydrogels from PVA-poly (acrylamide-co-acryloyl phenylalanine) and their antimicrobial studies. Bull. Korean Chem. Soc, 2012. 33(10): p. 3191.
38. Abd El Wahab, R.M., et al., Assessment of a green zeolite/bacterial cellulose nanocomposite membrane as a catalyst to produce biodiesel from waste cooking oil. Energy Sources, Part A: Recovery, Utilization, and Environmental Effects, 2023. 45(4): p. 10350-10365.
39. Tarasova, N., et al., The new approach to the preparation of polyacrylamide-based hydrogels: Initiation of polymerization of acrylamide with 1, 3-dimethylimidazolium (phosphonooxy-) oligosulphanide under drying aqueous solutions. Polymers, 2021. 13(11): p. 1806.
40. Šimon, E.K.-P.Š.-P. and A. Gatial, Confirmation of polymerisation effects of sodium chloride and its additives on acrylamide by infrared spectrometry. Journal of Food and Nutrition Research, 2007. 46(1): p. 39-44.
41. Kumar, P., et al., Novel high-viscosity polyacrylamidated chitosan for neural tissue engineering: fabrication of anisotropic neurodurable scaffold via molecular disposition of persulfate-mediated polymer slicing and complexation. International journal of molecular sciences, 2012. 13(11): p. 13966-13984.
42. Nazarenko, O. and R. Zarubina, Application of sakhaptinsk zeolite for improving the quality of ground water. Energy and Environmental Engineering, 2013. 1(2): p. 68-73.
43. Sugahara, Y., et al., Preparation of a kaolinite-polyacrylamide intercalation compound. clays and clay Minerals, 1990. 38(2): p. 137-143.
44. Deng, Y., et al., Bonding between polyacrylamide and smectite. Colloids and Surfaces A: Physicochemical and Engineering Aspects, 2006. 281(1-3): p. 82-91.
45. Ramírez, A., et al., Characterization and Modification of Red Mud and Ferrosilicomanganese Fines and Their Application in the Synthesis of Hybrid Hydrogels. Polymers, 2022. 14(20): p. 4330.
46. Radoor, S., et al., Efficient removal of methyl orange from aqueous solution using mesoporous ZSM-5 zeolite: Synthesis, kinetics and isotherm studies. Colloids and Surfaces A: Physicochemical and Engineering Aspects, 2021. 611: p. 125852.
47. Mallakpour, S. and S. Rashidimoghadam, Poly (vinyl alcohol)/Vitamin C-multi walled carbon nanotubes composites and their applications for removal of methylene blue: Advanced comparison between linear and nonlinear forms of adsorption isotherms and kinetics models. Polymer, 2019. 160: p. 115-125.
48. Oyarce, E., et al., Adsorption of methylene blue in aqueous solution using hydrogels based on 2-hydroxyethyl methacrylate copolymerized with itaconic acid or acrylic acid. Materials Today Communications, 2020. 25: p. 101324.
49. Badawy, A.A., S.M. Ibrahim, and H.A. Essawy, Enhancing the textile dye removal from aqueous solution using cobalt ferrite nanoparticles prepared in presence of fulvic acid. Journal of Inorganic and Organometallic Polymers and Materials, 2020. 30(5): p. 1798-1813.
50. Bulut, Y. and H. Aydın, A kinetics and thermodynamics study of methylene blue adsorption on wheat shells. Desalination, 2006. 194(1-3): p. 259-267.
51. Ao, D., L. AP, and O. AM, Langmuir, Freundlich, Temkin and Dubinin–Radushkevich isotherms studies of equilibrium sorption of Zn 2+ unto phosphoric acid modified rice husk. IOSR Journal of applied chemistry, 2012. 3(1): p. 38-45.
52. Hu, Q. and Z. Zhang, Application of Dubinin–Radushkevich isotherm model at the solid/solution interface: A theoretical analysis. Journal of Molecular Liquids, 2019. 277: p. 646-648.
53. Hidayat, E., et al., Methylene blue removal by chitosan cross-linked zeolite from aqueous solution and other ion effects: Isotherm, kinetic, and desorption studies. Adsorption Science & Technology, 2022. 2022: p. 1853758.
54. Ramezani, H., S.N. Azizi, and G. Cravotto, Improved removal of methylene blue on modified hierarchical zeolite Y: Achieved by a “destructive-constructive” method. Green Processing and Synthesis, 2019. 8(1): p. 730-741.
55. Picón, D., et al., Adsorption of methylene blue and tetracycline by zeolites immobilized on a PBAT electrospun membrane. Molecules, 2022. 28(1): p. 81.
56. Ibrahim, M.A., et al., Fabrication of cellulose nanocrystals /carboxymethyl cellulose /zeolite membranes for methylene blue dye removal: understanding factors, adsorption kinetics, and thermodynamic isotherms. Frontiers in Chemistry, 2024. 12: p. 1330810.
57. Peng, S., et al., Ionic polyacrylamide hydrogel improved by graphene oxide for efficient adsorption of methylene blue. Research on Chemical Intermediates, 2019. 45: p. 1545-1563.

58. Dai, H., Y. Huang, and H. Huang, Eco-friendly polyvinyl alcohol/carboxymethyl cellulose hydrogels reinforced with graphene oxide and bentonite for enhanced adsorption of methylene blue. Carbohydrate polymers, 2018. 185: p. 1-11.
59. Mohammadzadeh, F., et al., Adsorption kinetics of methylene blue from wastewater using pH-sensitive starch-based hydrogels. Scientific Reports, 2023. 13(1): p. 11900.
60. Cheng, Z., et al., Adsorption kinetic character of copper ions onto a modified chitosan transparent thin membrane from aqueous solution. Journal of Hazardous Materials, 2010. 182(1-3): p. 408-415.
61. Al-Odayni, A.-B., F.S. Alsubaie, and W.S. Saeed, Nitrogen-rich polyaniline-based activated carbon for water treatment: adsorption kinetics of anionic dye methyl orange. Polymers, 2023. 15(4): p. 806.
62. Mashkoor, F. and A. Nasar, Magnetized Tectona grandis sawdust as a novel adsorbent: preparation, characterization, and utilization for the removal of methylene blue from aqueous solution. Cellulose, 2020. 27(5): p. 2613-2635.
63. Benturki, O., et al., Synthesis and characterization of activated carbons obtained from jujube shells "Nebka". J. Soc. Alger. Chim, 2008. 18(1): p. 7-23.
64. Bouhdadi, R., et al., Chemical modification of cellulose by acylation: Application to adsorption of methylene blue. Maderas. Ciencia y tecnología, 2011. 13(1): p. 105-116.
65. Prajaputra, V., et al. Characterization of Na-P1 zeolite synthesized from pumice as low-cost materials and its ability for methylene blue adsorption. in IOP Conference Series: Earth and Environmental Science. 2019. IOP Publishing.
66. Sagita, C.P., L. Nulandaya, and Y.S. Kurniawan, Efficient and low-cost removal of methylene blue using activated natural kaolinite material. Journal of Multidisciplinary Applied Natural Science, 2021. 1(2): p. 69-77.
67. Tran, H.N., et al., Insight into the adsorption mechanism of cationic dye onto biosorbents derived from agricultural wastes. Chemical Engineering Communications, 2017. 204(9): p. 1020-1036.
68. Kim, H.-J., et al., Zero discharge of dyes and regeneration of a washing solution in membrane-based dye removal by cold plasma treatment. Membranes, 2022. 12(6): p. 546.
69. Jalal, A.F. and N.A. Fakhre, Removal of dyes (BG, MG, and SA) from aqueous solution using a novel adsorbent macrocyclic compound. Plos one, 2022. 17(10): p. e0275330.